JTAM (Jurnal Teori dan Aplikasi Matematika)
http://journal.ummat.ac.id/index.php/jtam
p-ISSN 2597-7512 | e-ISSN 2614-1175
Vol. 8, No. 4, October 2024, pp. 1067-1081

Mathematical Model of COVID-19 Spread with Vaccination in Mataram City

Muhammad Putra Sani Hattamurrahman[1], Paian Sianturi[1], Hadi Sumarno[1]
[1]Department of Mathematics, IPB University, Indonesia
sanihatta98@gmail.com

Article History:
Received : 30-04-2024
Revised : 20-07-2024
Accepted : 22-07-2024
Online : 01-10-2024

Keywords:
COVID-19;
Vaccination;
Mathematical model;
Basic reproduction number;
Routh Hurwitz criterion;
Lyapunov function;
Mathematical model.

ABSTRACT

The COVID-19 pandemic has had a significant impact on public health worldwide. Mathematical modeling is considered an alternative tool for understanding real-life problems, including the dynamics of COVID-19 spread. This is an applied research that purpose adds vaccination to SEIQR model of COVID-19 spread and examines the dynamic of COVID-19 spread in Mataram City. First, we construct the new model by making assumptions. The fixed point and basic reproduction number ($\mathcal{R}_0$) are then used to analyze the model using the next-generation matrix method. The next-generation matrix method is utilized to estimate the $\mathcal{R}_0$ in a compartmental disease model. Two fixed points are acquired, specifically the disease-free fixed point, which is locally asymptotically stable under the condition $\mathcal{R}_0 < 1$ determined by the Routh Hurwitz criterion via linearization using the Jacobi matrix. And the disease-endemic fixed point, which is locally asymptotically stable under the condition $\mathcal{R}_0 > 1$ indicated by Lyapunov function. The population dynamics when $\mathcal{R}_0 < 1$ and $\mathcal{R}_0 > 1$ can also be observed through numerical simulation. The results of a numerical simulation indicate that giving the proportion of number vaccinated 62 per cent is effective in suppressing the number of infections.

https://doi.org/10.31764/jtam.v8i4.23113

A. INTRODUCTION

SARS-COV-2 (Severe Actue Respiratory Syndrome Coronavirus 2) is the coronavirus that causes COVID-19, a respiratory disease. It spreads through saliva droplets released when an infected person coughs or sneezes (Hardianti et al., 2022; N. Zhu et al., 2020). The COVID-19 outbreak has had a significant negative impact on society and the economy in addition to affecting public health (Polwiang, 2023). COVID-19 was first detailed in Wuhan, China in December 2019 (Naresh et al., 2023). More than 499 million confirmed cases of COVID-19, including more than 6 million deaths worldwide, were reported on April 13, 2022 (Wang et al., 2022).As indicated by information detailed by the World Health Organization (WHO), internationally, as of August 30, 2023, there were 770,085,713 affirmed instances of Coronavirus, including 6,956,173 passings.

WHO declared COVID-19 a pandemic due to its high transmission rate (Rahmasari et al., 2023). Researchers are deeply concerned about the spread of this coronavirus disease because of the rising number of cases and the high mortality rate worldwide (Naresh et al., 2023). The spread of the disease is tracked by researchers using mathematical models (I. U. Khan et al.,

2023). By using mathematical models, researcher can focus on investigating the dynamics of diseases that are contagious and spread throughout the population and become an important tool for establishing good strategies to fight this pandemic (Verma et al., 2023). In recent developments (Abidemi et al., 2023), a few mathematicians have utilized numerical models with memory records to evaluate the elements of sickness transmission (Naresh et al., 2023).

There are also studies to forecast future COVID-19 with SIR, SEIR and SEIQR models (Cheruku et al., 2023; Hassan et al., 2023; Rahimi et al., 2021). Cao et al. (2020) looked at the coronavirus's clinical characteristics and the short-term outcomes of 18 and 102 COVID-19 patients in the intensive care unit. Ming et al. (2020) presented a modified SIR epidemic model to project the number of infected patients and the specific burden in intensive care units and isolation wards. A SIR epidemic model (susceptible, infected, and recovered) was developed by Nesteruk (2020) and he also discussed the statistics of the parameters used in the model and demonstrated how to control the infection. Other studies cope with the implementation of lockdowns and vaccines (Polwiang, 2023) and with the use of masks (DarAssi et al., 2023).

A model created by Zeb et al. (2020) is the basis for this study. The goal of the model is to demonstrate the changing patterns of COVID-19 by incorporating isolation categories. Assessing both local and global stability is achieved by utilizing the fundamental reproductive number. Next, the numerical solution will be achieved by applying a Non-Standard Finite Difference Scheme (NSFD) in combination with the 4th order Runge-Kutta method…. Zeb et al. (2020) findings indicate that COVID-19 can be spread through human contact. As a result, the risk of COVID-19 spreading in the future can be reduced by isolating exposed and infected humans. In any case, in a few different examinations, it was referenced that resistance after recuperation is impermanent; people will lose invulnerability so they will get back to being a weak subpopulation (Bjørnstad et al., 2020; Margenov et al., 2022; Singh et al., 2022).

This study also involved additional vaccine subgroups, dependent on vaccine data accessibility in Mataram city. By analyzing the stability of fixed points and using daily data of COVID-19 patients in Mataram City, researcher aim to create a model and assess how vaccination impacts the transmission of the virus. Researcher anticipates that introducing the vaccine subpopulation will help educate the public on the significance of getting vaccinated. Additionally, through fixed point stability analysis, they hope to offer guidance to the government in shaping future policies to combat the spread of COVID-19.

B. METHODS

The following steps were followed during the literature review phase of this study:

1. Modify the SEIQR model developed by Zeb et al. (2020) to reassemble the COVID-19 disease spread model.
2. Collect daily data on COVID-19 in Mataram city from November 1, 2020, to April 30, 2021. The data was obtained by visiting Dinas Kesehatan West Nusa Tenggara Province, and then based on the data obtained, parameters that were actually related to the model were selected and processed using Excel.
3. Determine the disease-free fixed point and endemic fixed point of the model using of the Routh-Hurwitz criterion and Lyapunov function.
4. Utilizing the next generation matrix, determine the base reproduction number($\mathcal{R}_0$).

5. Utilize the actual data from COVID-19 patients in Mataram city to determine the parameter values.
6. Real data on COVID-19 patients in Mataram City can be used to run numerical simulations of the model.

SEIQR Model by Zeb: Zeb Model is broken down into five subpopulations: susceptible (S), exposed (E), infected (I), quarantined (Q) and recovered from the disease (R). The assumption is used in the models are the mortality and birth rates are equal and individuals who are exposed and infected are having interactions with each other. Furthermore, a new isolation class (Q) has been added to the model. Based on assumptions, the diagram by Zeb can be seen in Figure 1.

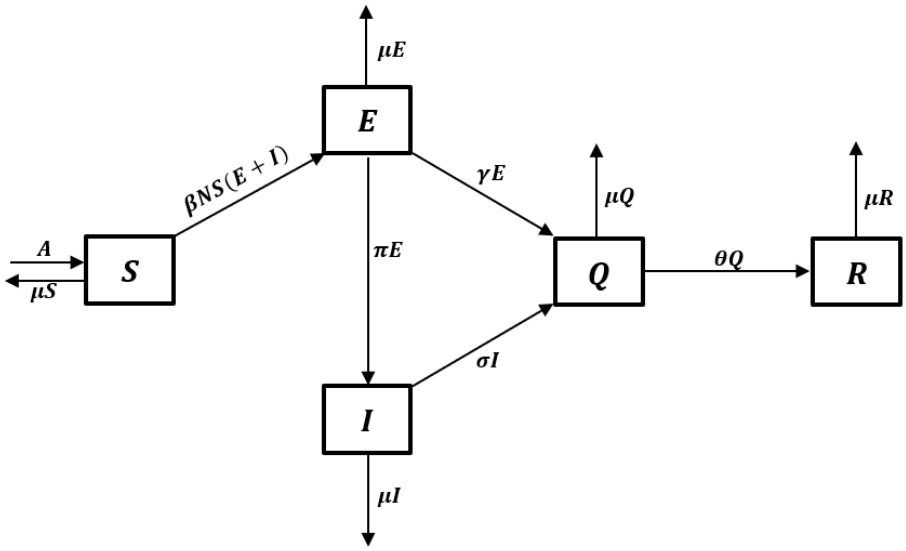

Figure 1. COVID-19 disease spread diagram by Zeb

The following is the model formed by Zeb based on Figure 1.

$$\frac{dS(t)}{dt} = A - \mu S(t) - \beta NS(t)[E(t) + I(t)]$$
$$\frac{dE(t)}{dt} = \beta NS(t)[E(t) + I(t)] - \pi E(t) - (\mu + \gamma)E(t)$$
$$\frac{dI(t)}{dt} = \pi E(t) - \sigma I(t) - \mu I(t)$$
$$\frac{dQ(t)}{dt} = \gamma E(t) + \sigma I(t) - \theta Q(t) - \mu Q(t)$$
$$\frac{dR(t)}{dt} = \theta Q(t) - \mu R(t)$$

Where $A, \mu, \beta, N, \pi, \gamma, \sigma, \theta > 0$. The description of each parameter is: N is total population; A is the rate of births; μ is natural death rate;β is conversion rate from susceptible to exposed subpopulation;π is conversion rate from exposed to infected subpopulation; γ is conversion rate from exposed to quarantine subpopulation; σ is conversion rate from infected to quarantine subpopulation; and θ is conversion rate from quarantined to recovered subpopulation.

C. RESULT AND DISCUSSION

1. Mathematical Model

Modifications to the mathematical model of the spread of COVID-19 containing quarantine classes (Zeb et al., 2020) are by adding vaccine subpopulations (Diagne et al., 2021; Resmawan et al., 2022; Septiansyah et al., 2022) and assuming individuals who have recovered can become susceptible again (Bjørnstad et al., 2020; Margenov et al., 2022; Singh et al., 2022). In addition, individuals from vaccinated subpopulations may become recovered (Peter et al., 2023; Pinto Neto et al., 2021). The presumptions utilized in this study are as per the following:

a. Six subpopulations comprise the group: susceptible (S), exposed (E), infected (I), quarantine (Q), recovered (R) and vaccine (V) subpopulations.
b. Through contact with the exposed subpopulation (E) and the infected subpopulation (I), the susceptible subpopulation (S) can be exposed to the virus.
c. Individuals in the susceptible subpopulation will join to the vaccine subpopulation at a rate η.
d. Individuals in the vaccinated subpopulation will join to the recovered subpopulation at a rate ξ.
e. Individuals who have recovered, whether vaccinated or not, can return to the susceptible subpopulation due to loss of immunity at a rate of δ.
f. The natural mortality rate and and the birth rate are symbolized by μ.

Schematically, based on the above description, the following subpopulation diagram can illustrate the model to be created.

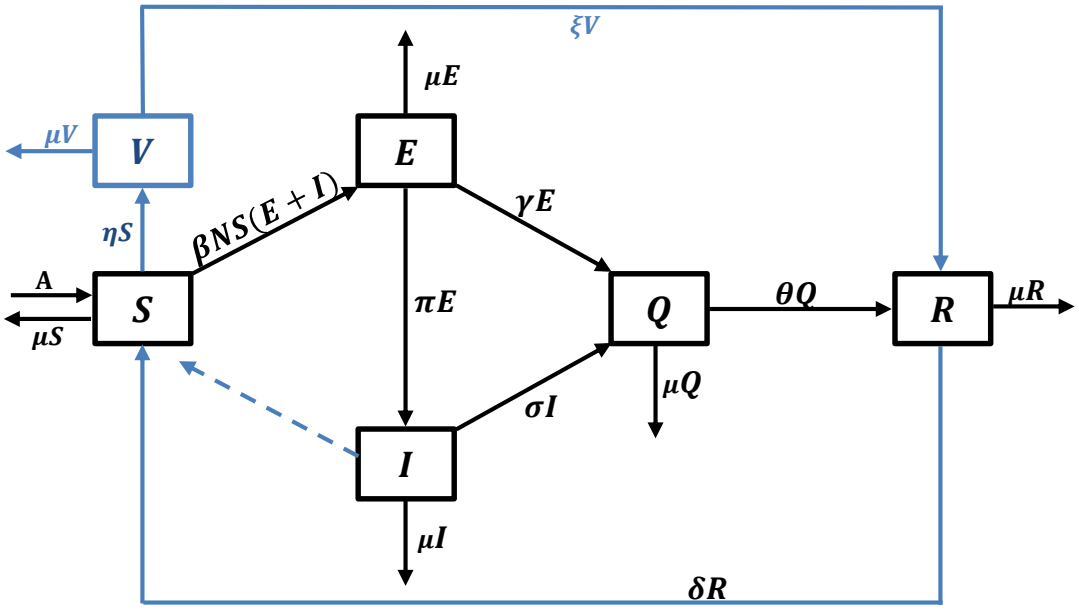

Figure 2. COVID-19 disease spread diagram (adopted from Zeb)

The following is the model obtained based on the diagram in Figure 2.

$$\begin{aligned}
\frac{dS(t)}{dt} &= \mathrm{A} + \delta R(t) - (\eta + \mu)S(t) - \beta NS(t)[E(t) + I(t)] \\
\frac{dE(t)}{dt} &= \beta NS(t)[E(t) + I(t)] - (\mu + \pi + \gamma)E(t) \\
\frac{dI(t)}{dt} &= \pi E(t) - (\mu + \sigma)I(t) \\
\frac{dQ(t)}{dt} &= \gamma E(t) + \sigma I(t) - (\mu + \theta)Q(t) \\
\frac{dR(t)}{dt} &= \theta Q(t) + \xi V(t) - (\mu + \delta)R(t) \\
\frac{dV(t)}{dt} &= \eta S(t) - (\mu + \xi)V(t)
\end{aligned} \tag{1}$$

where $\mu, \delta, \eta, \xi > 0$ and $N = S(t) + E(t) + I(t) + Q(t) + R(t) + V(t)$. The parameters are described as follows: μ is birth and natural death rates; δ is Rate of loss of immunity from recovered to susceptible subpopulation; η is Proportion of number vaccinated; and ξ is Rate of vaccinated become recovered. To make proportions in the system of equations (3.1) above, the variables (S, E, I, Q, R, V) are expressed in the following form.

$$\mu = \frac{\mathrm{A}}{N}, s = \frac{S}{N}, e = \frac{E}{N}, i = \frac{I}{N}, q = \frac{Q}{N}, r = \frac{R}{N}, v = \frac{V}{N}$$

As a result, system (1) can be rewritten as follows.

$$\begin{aligned}
\frac{ds}{dt} &= \mu + \delta r - (\eta + \mu)s - \beta\, N\, s\, (e + i) \\
\frac{de}{dt} &= \beta\, N\, s\, (e + i) - (\mu + \pi + \gamma)e \\
\frac{di}{dt} &= \pi e - (\mu + \sigma)i \\
\frac{dq}{dt} &= \gamma e + \sigma i - (\mu + \theta)q \\
\frac{d\, r}{dt} &= \theta q + \xi v - (\mu + \delta)\, r \\
\frac{dv}{dt} &= \eta s - (\mu + \xi)v
\end{aligned} \tag{2}$$

Henceforth, the system of equations (2) is used in the analysis.

2. Fixed Point of the Model

To determine the fixed point is done by solving equation (2) and fulfilling the condition

$$\frac{\boldsymbol{ds}}{\boldsymbol{dt}} = \frac{\boldsymbol{de}}{\boldsymbol{dt}} = \frac{\boldsymbol{di}}{\boldsymbol{dt}} = \frac{\boldsymbol{dq}}{\boldsymbol{dt}} = \frac{\boldsymbol{dr}}{\boldsymbol{dt}} = \frac{\boldsymbol{dv}}{\boldsymbol{dt}} = \mathbf{0} \tag{3}$$

Based on equation 3, The endemic fixed point and the disease-free fixed point are the two outcomes. A disease-free fixed point is a situation in which a given population does not have any diseases. If $e = i = q = 0$, the disease-free fixed point is found. In order to obtain the disease-free fixed point, follow these steps:

$$T_0(s, e, i, q, r, v) = (s^0, 0,0,0, r^0, v^0) \tag{4}$$

with

$$s^0 = \frac{(\mu+\delta)(\mu+\xi)}{(\eta+\mu)(\mu+\xi)+\delta(\eta+\mu+\xi)}$$

$$r^0 = \frac{\eta\xi}{(\eta+\mu)(\mu+\xi)+\delta(\eta+\mu+\xi)}$$

$$v^0 = \frac{\eta(\mu+\delta)}{(\eta+\mu)(\mu+\xi)+\delta(\eta+\mu+\xi)}$$

An endemic fixed point is a condition in which a particular population still has infected individuals. The system of equations (2) gives the disease fixed point as follows.

$$T_1(s,e,i,q,r,v) = (s^*,e^*,i^*,q^*,r^*,v^*) \tag{5}$$

with

$$s^* = \frac{\mu+\delta r}{\beta N(e+i)+\eta+\mu}$$

$$e^* = -\frac{\beta N s i}{\beta N s-(\mu+\pi+\gamma)}$$

$$i^* = \frac{\pi e}{\mu+\sigma}$$

$$q^* = \frac{\gamma e+\sigma i}{\theta+\mu}$$

$$r^* = \frac{\theta q+\xi v}{\mu+\delta}$$

$$v^* = \frac{\eta s}{\mu+\xi}$$

Then, linearization will be carried out using the Jacobian matrix.

3. Jacobian Matrix

Suppose the system of equations (2) is written as follows.

$$\begin{aligned}
\frac{ds}{dt} &= \boldsymbol{f_1(s,e,i,q,r,v) = \mu + \delta r - (\eta + \mu)s - \beta N s(e+i)} \\
\frac{de}{dt} &= \boldsymbol{f_2(s,e,i,q,r,v) = \beta N s(e+i) - (\mu + \pi + \gamma)e} \\
\frac{di}{dt} &= \boldsymbol{f_3(s,e,i,q,r,v) = \pi e - (\mu + \sigma)i} \\
\frac{dq}{dt} &= \boldsymbol{f_4(s,e,i,q,r,v) = \gamma e + \sigma i - (\mu + \theta)q} \\
\frac{dr}{dt} &= \boldsymbol{f_5(s,e,i,q,r,v) = \theta q + \xi v - (\mu + \delta)\, r} \\
\frac{dv}{dt} &= f_6(s,e,i,q,r,v) = \eta s - (\mu + \xi)v
\end{aligned} \tag{6}$$

The Jacobi matrix can be obtained in the following manner by linearizing the equation system (6)

$$J = \begin{pmatrix}
\frac{\partial f_1}{\partial s} & \frac{\partial f_1}{\partial e} & \frac{\partial f_1}{\partial i} & \frac{\partial f_1}{\partial q} & \frac{\partial f_1}{\partial r} & \frac{\partial f_1}{\partial v} \\
\frac{\partial f_2}{\partial s} & \frac{\partial f_2}{\partial e} & \frac{\partial f_2}{\partial i} & \frac{\partial f_2}{\partial q} & \frac{\partial f_2}{\partial r} & \frac{\partial f_2}{\partial v} \\
\frac{\partial f_3}{\partial s} & \frac{\partial f_3}{\partial e} & \frac{\partial f_3}{\partial i} & \frac{\partial f_3}{\partial q} & \frac{\partial f_3}{\partial r} & \frac{\partial f_3}{\partial v} \\
\frac{\partial f_4}{\partial s} & \frac{\partial f_4}{\partial e} & \frac{\partial f_4}{\partial i} & \frac{\partial f_4}{\partial q} & \frac{\partial f_4}{\partial r} & \frac{\partial f_4}{\partial v} \\
\frac{\partial f_5}{\partial s} & \frac{\partial f_5}{\partial e} & \frac{\partial f_5}{\partial i} & \frac{\partial f_5}{\partial q} & \frac{\partial f_5}{\partial r} & \frac{\partial f_5}{\partial v} \\
\frac{\partial f_6}{\partial s} & \frac{\partial f_6}{\partial e} & \frac{\partial f_6}{\partial i} & \frac{\partial f_6}{\partial q} & \frac{\partial f_6}{\partial r} & \frac{\partial f_6}{\partial v}
\end{pmatrix}$$

$$J = \begin{pmatrix}
-\beta N(e+i) - (\eta + \mu) & -\beta N s & -\beta N s & 0 & \delta & 0 \\
\beta N(e+i) & \beta N s - (\mu + \pi + \gamma) & \beta N s & 0 & 0 & 0 \\
0 & \pi & -(\mu + \sigma) & 0 & 0 & 0 \\
0 & \gamma & \sigma & -(\theta + \mu) & 0 & 0 \\
0 & 0 & 0 & \theta & -(\mu + \delta) & \xi \\
\eta & 0 & 0 & 0 & 0 & -(\mu + \xi)
\end{pmatrix}$$

4. Basic Reproduction Number

The disease's limit for spreading is the basic reproduction number, denoted by $\mathcal{R}_0$. This fundamental reproduction number is used to determine whether or not the disease is endemic. If $\mathcal{R}_0 > 1$, the disease will be endemic; otherwise, if $\mathcal{R}_0 < 1$, it will gradually disappear from the system (Abidemi et al., 2023). The next generation matrix method is used to determine the fundamental reproductive number. So from the system of equations (2) is obtained

$$\mathcal{F} = \begin{pmatrix} \beta N s(e+i) \\ 0 \end{pmatrix}, \mathcal{V} = \begin{pmatrix} (\mu + \pi + \gamma)e \\ -\pi e + (\mu + \sigma)i \end{pmatrix} \tag{7}$$

The matrix is then obtained by determining how each matrix element of F dan V relates to e and i

$$\boldsymbol{F} = \begin{pmatrix} \boldsymbol{\beta N \frac{(\mu+\delta)(\mu+\xi)}{(\eta+\mu)(\mu+\xi)+\delta(\eta+\mu+\xi)}} & \boldsymbol{\beta N \frac{(\mu+\delta)(\mu+\xi)}{(\eta+\mu)(\mu+\xi)+\delta(\eta+\mu+\xi)}} \\ \boldsymbol{0} & \boldsymbol{0} \end{pmatrix}, \boldsymbol{V} = \begin{pmatrix} \boldsymbol{\mu+\pi+\gamma} & \boldsymbol{0} \\ \boldsymbol{-\pi} & \boldsymbol{\mu+\sigma} \end{pmatrix}$$

Furthermore, the calculation using the next generation matrix approach is obtained using the following equation.

$$\boldsymbol{G = FV^{-1}}$$
$$\boldsymbol{G} = \begin{pmatrix} \boldsymbol{\beta N \frac{(\mu+\delta)(\mu+\xi)}{(\eta+\mu)(\mu+\xi)+\delta(\eta+\mu+\xi)}} & \boldsymbol{\beta N \frac{(\mu+\delta)(\mu+\xi)}{(\eta+\mu)(\mu+\xi)+\delta(\eta+\mu+\xi)}} \\ \boldsymbol{0} & \boldsymbol{0} \end{pmatrix} \begin{pmatrix} \boldsymbol{\mu+\pi+\gamma} & \boldsymbol{0} \\ \boldsymbol{-\pi} & \boldsymbol{\mu+\sigma} \end{pmatrix}^{\boldsymbol{-1}}$$

Hence, $\boldsymbol{\mathcal{R}_0}$ is the maximum eigenvalue of matrix G, which is

$$\boldsymbol{\mathcal{R}_0} = \frac{\boldsymbol{\beta N(\mu+\delta)(\mu+\xi)}}{\boldsymbol{((\eta+\mu)(\mu+\xi)+\delta(\eta+\mu+\xi))(\mu+\pi+\gamma)}} \tag{8}$$

Theorem 1 (Disease-Free Fixed Point Stability)
The disease-free fixed point in equation (4) is locally asymptotically stable if $\mathcal{R}_0 < 1$ (Van Den Driessche & Watmough, 2002).

Proof.
Using the basic reproduction number obtained in the previous stage, we will now examine the stability requirements of the disease-free fixed point in accordance with Theorem 1. Linearization at the fixed point T_0 will result in the following Jacobi matrix

$$J_{T_0} = \begin{pmatrix} -(\eta+\mu) & -\beta N s^0 & -\beta N s^0 & 0 & \delta & 0 \\ 0 & \beta N s^0 - (\mu+\pi+\gamma) & \beta N s^0 & 0 & 0 & 0 \\ 0 & \pi & -(\mu+\sigma) & 0 & 0 & 0 \\ 0 & \gamma & \sigma & -(\theta+\mu) & 0 & 0 \\ 0 & 0 & 0 & \theta & -(\mu+\delta) & \xi \\ \eta & 0 & 0 & 0 & 0 & -(\mu+\xi) \end{pmatrix}$$

The characteristic equation is used to calculate the eigenvalues derived from J_{T_0}, i.e.

$$\big(\lambda+(\eta+\mu)\big)\big(\lambda+(\theta+\mu)\big)\big(\lambda+(\mu+\delta)\big)\big(\lambda+(\mu+\xi)\big)(\lambda^2+C_1\lambda+C_2) = 0 \tag{9}$$

With

$$\boldsymbol{C_1 = -\beta N s^0 + (\mu+\pi+\gamma) + (\mu+\sigma)}$$
$$C_2 = (-\beta N s^0 + (\mu+\pi+\gamma))(\mu+\sigma) - \pi(\mu+\sigma)$$

Based on equation (9), six eigenvalues are obtained, i.e. $\lambda_1 = -\eta-\mu, \lambda_2 = -\theta-\mu, \lambda_3 = -\mu-\delta, \lambda_4 = -\mu-\xi$ and its two eigenvalues are obtained using the following equation.

$$(\lambda^2 + C_1\lambda + C_2) = 0$$

The fixed point T_0 will be stable if and only if the stability conditions $C_1 > 0$ and $C_2 > 0$ are met, according to the Routh-Hurwitz criterion.

Proof.
The characteristic equation will then be proven to meet the stability requirements of the Routh-Hurwitz criterion. Based on the results of parameter calculations where all are positive, then C_1 and C_2 are also positive. The calculation can be seen as follows.
If $\boldsymbol{\mathcal{R}_0 < 1}$ is locally asymptotically stable then

$$\begin{gathered}\frac{\boldsymbol{\beta N(\mu+\delta)(\mu+\xi)}}{\boldsymbol{((\eta+\mu)(\mu+\xi)+\delta(\eta+\mu+\xi))(\mu+\pi+\gamma)}} < \mathbf{1} \\ \frac{\boldsymbol{\beta N s^0}}{\boldsymbol{(\mu+\pi+\gamma)}} < \mathbf{1} \\ \boldsymbol{-\beta N s^0 + (\mu+\pi+\gamma) > 0}\end{gathered} \tag{6}$$

$$\boldsymbol{C_1 = -\beta N s^0 + (\mu+\pi+\gamma) + (\mu+\sigma)}$$

or can be written into

$$\boldsymbol{C_1 = (1-\mathcal{R}_0)(\mu+\pi+\gamma) + (\mu+\sigma)}$$

Based on equation (10) and the positive values of parameters $\boldsymbol{(\mu+\pi+\gamma)}$ and $\boldsymbol{(\mu+\sigma)}$ and the condition that $\boldsymbol{\mathcal{R}_0 < 1, C_1 > 0}$.

$$\boldsymbol{C_2 = -\beta N s^0 + (\mu+\pi+\gamma))(\mu+\sigma) - \pi(\mu+\sigma)}$$

or can be written into

$$\boldsymbol{C_2 = (1-\mathcal{R}_0)(\mu+\pi+\gamma)(\mu+\sigma)(1-\pi)}$$

Based on equation (10), with positive values of parameters $\boldsymbol{(\mu+\sigma)}$ and $\boldsymbol{(1-\pi)}$ and with the condition that $\boldsymbol{\mathcal{R}_0 < 1, C_2 > 0}$. It is clear that the eigenvalues of J_{T_0} have negative real parts when $C_1, C_2 > 0$, as can be seen from the above explanation, which is an application of the Routh-Hurwitz criterion. Hence the other two eigenvalues, $\lambda_5 < 0$ and $\lambda_6 < 0$. Therefore, the disease-free fixed point is unstable if $\mathcal{R}_0 > 1$ and locally asymptotically stable if $\mathcal{R}_0 < 1$.

Theorem 2 (Endemic Fixed Point Stability)
The endemic fixed point in equation (4) is globally asymptotically stable if $\mathcal{R}_0 > 1$ (Salle & Lefschetz, 1961).

Proof.
Define the Lyapunov function L: $\mathbb{R}^6 \to \mathbb{R}$ with the following formula. The following Lyapunov function is called a quadratic Lyapunov function, with each coefficient m_i as a scale factor.

$$L(s,e,i,q,r,v) = \frac{m_1(s-s^*)}{2} + \frac{m_2(e-e^*)}{2} + \frac{m_3(i-i^*)}{2} + \frac{m_4(q-q^*)}{2} + \frac{m_5(r-r^*)}{2} + \frac{m_6(v-v^*)}{2}$$

Since the function L consists of polynomial functions, it is obvious that L is continuous. Then,

$$\frac{dL}{dt} = m_1(s-s^*)\frac{ds}{dt} + m_2(e-e^*)\frac{de}{dt} + m_3(i-i^*)\frac{di}{dt} + m_4(q-q^*)\frac{dq}{dt} + m_5(r-r^*)\frac{dr}{dt} + m_6(v-v^*)\frac{dv}{dt}$$

By substituting the system of equations (2) then

$$\begin{aligned}\frac{dL}{dt} = {} & m_1(s-s^*)[\mu + \delta r - (\eta+\mu)s - \beta N s(e+i)] \\ & + m_2(e-e^*)[\beta N s(e+i) - (\mu+\pi+\gamma)e] + m_3(i-i^*)[\pi e - (\mu+\sigma)i] \\ & + m_4(q-q^*)[\gamma e + \sigma i - (\mu+\theta)q] + m_5(r-r^*)[\theta q + \xi v - (\mu+\delta)r] \\ & + m_6(v-v^*)[\eta s - (\mu+\xi)v]\end{aligned}$$

Given that at the endemic fixed point the system (6) applies, thus

$$\begin{aligned}\frac{dL}{dt} = {} & m_1(s-s^*)\big[[\mu + \delta r - (\eta+\mu)s - \beta N s(e+i)] \\ & - [\mu + \delta r - (\eta+\mu)s^* - \beta N s^*(e^*+i^*)]\big] \\ & + m_2(e-e^*)\big[[\beta N s(e+i) - (\mu+\pi+\gamma)e] \\ & - [\beta N s^*(e^*+i^*) - (\mu+\pi+\gamma)e^*]\big] \\ & + m_3(i-i^*)\big[[\pi e - (\mu+\sigma)i] - [\pi e^* - (\mu+\sigma)i^*]\big] \\ & + m_4(q-q^*)\big[[\gamma e + \sigma i - (\mu+\theta)q] - [\gamma e^* + \sigma i^* - (\mu+\theta)q^*]\big] \\ & + m_5(r-r^*)\big[[\theta q + \xi v - (\mu+\delta)r] - [\theta q^* + \xi v^* - (\mu+\delta)r^*]\big] + m_6(v \\ & - v^*)\big[[\eta s - (\mu+\xi)v] - [\eta s^* - (\mu+\xi)v^*]\big] \\ \frac{dL}{dt} = {} & m_1(s-s^*)[-(\eta+\mu)s - \beta N s(e+i) + (\eta+\mu)s^* + \beta N s^*(e^*+i^*)] \\ & + m_2(e-e^*)[\beta N s(e+i) - (\mu+\pi+\gamma)e - \beta N s^*(e^*+i^*) + (\mu+\pi+\gamma)e^*] \\ & + m_3(i-i^*)[\pi e - (\mu+\sigma)i - \pi e^* + (\mu+\sigma)i^*] \\ & + m_4(q-q^*)[\gamma e + \sigma i - (\mu+\theta)q - \gamma e^* - \sigma i^* + (\mu+\theta)q^*] \\ & + m_5(r-r^*)[\theta q + \xi v - (\mu+\delta)r - \theta q^* - \xi v^* + (\mu+\delta)r^*] + m_6(v \\ & - v^*)[\eta s - (\mu+\xi)v - \eta s^* + (\mu+\xi)v^*] \\ \frac{dL}{dt} = {} & m_1(s-s^*)\big[-(\eta+\mu)(s-s^*) - \beta N\big(s(e+i) - s^*(e^*+i^*)\big)\big] \\ & + m_2(e-e^*)\big[\beta N\big(s(e+i) - s^*(e^*+i^*)\big) - (\mu+\pi+\gamma)(e-e^*)\big] \\ & + m_3(i-i^*)[\pi(e-e^*) - (\mu+\sigma)(i-i^*)] \\ & + m_4(q-q^*)[\gamma(e-e^*) + \sigma(i-i^*) - (\mu+\theta)(q-q^*)] \\ & + m_5(r-r^*)[\theta(q-q^*) + \xi(v-v^*) - (\mu+\delta)(r-r^*)] + m_6(v \\ & - v^*)[\eta(s-s^*) - (\mu+\xi)(v-v^*)]\end{aligned}$$

$$\frac{dL}{dt} = m_1(s-s^*)(s-s^*)\left[-(\eta+\mu) - \frac{\beta N\big(s(e+i)+s^*(e^*+i^*)\big)}{(s-s^*)}\right]$$
$$+ m_2(e-e^*)(e-e^*)\left[\frac{\beta N\big(s(e+i)-s^*(e^*+i^*)\big)}{(e-e^*)} - (\mu+\pi+\gamma)\right]$$
$$+ m_3(i-i^*)(i-i^*)\left[\frac{\pi(e-e^*)}{(i-i^*)} - (\mu+\sigma)\right]$$
$$+ m_4(q-q^*)(q-q^*)\left[\frac{\gamma(e-e^*)+\sigma(i-i^*)}{(q-q^*)} - (\mu+\theta)\right]$$
$$+\ m_5(r-r^*)(r-r^*)\left[\frac{\theta(q-q^*)+\xi(v-v^*)}{(r-r^*)} - (\mu+\delta)\right] + m_6(v-v^*)(v$$
$$-v^*)\left[\frac{\eta(s-s^*)}{(v-v^*)} - (\mu+\xi)\right]$$

By simplifying and removing the negative sign from the brackets in the equation above, we get

$$\frac{dL}{dt} = -m_1(s-s^*)^2\left[(\eta+\mu) + \frac{\beta N\big(s(e+i)+s^*(e^*+i^*)\big)}{(s-s^*)}\right]$$
$$- m_2(e-e^*)^2\left[-\frac{\beta N\big(s(e+i)-s^*(e^*+i^*)\big)}{(e-e^*)} + (\mu+\pi+\gamma)\right]$$
$$- m_3(i-i^*)^2\left[-\frac{\pi(e-e^*)}{(i-i^*)} + (\mu+\sigma)\right]$$
$$- m_4(q-q^*)^2\left[-\frac{\gamma(e-e^*)+\sigma(i-i^*)}{(q-q^*)} + (\mu+\theta)\right]$$
$$-\ m_5(r-r^*)^2\left[-\frac{\theta(q-q^*)+\xi(v-v^*)}{(r-r^*)} + (\mu+\delta)\right]$$
$$- m_6(v-v^*)^2\left[-\frac{\eta(s-s^*)}{(v-v^*)} + (\mu+\xi)\right]$$

Thus it is possible to choose non-negative m_1, m_2, m_3, m_4, m_5 and m_6 such that $\frac{dL}{dt} \leq 0$ is obtained under the condition that $\mathcal{R}_0 > 1$ (the condition for the existence of endemic fixed points) so that L is a Lyapunov function. Furthermore, $\frac{dL}{dt}$ is 0 when $s = s^*, e = e^*, i = i^*, q = q^*, r = r^*$ and $v = v^*$ that is when the fixed point is endemic. Thus, the largest invariant is the endemic fixed point $T_1(s^*, e^*, i^*, q^*, r^*, v^*)$ nd according to the Lyapunov-La Salle invariance principle, the endemic fixed point (3) is globally asymptotically stable on $\mathbb{R}_+^6$ when $\mathcal{R}_0 > 1$.

5. Numerical Simulation

Mathematica 13.2 software is used in this study's numerical simulation to display the stability of each fixed point by entering its parameter values into Table 1. Numerical simulations aim to show graphically that the fixed points obtained are locally when $\mathcal{R}_0 < 1$ and globally asymptotically stable when $\mathcal{R}_0 > 1$. It is known that the total population of Mataram city in NTB Province in 2020 is 495681, which is divided into several subpopulations. The initial values of these subpopulations were obtained from daily data on COVID-19 patients in the city

of Mataram, on November 1, 2020, in proportional form namely s^0 =0.2501, e^0=0.0003, i^0=0.0026, q^0=0.0002, r^0=0.0022 and v^0=0.7446.

Table 1. Parameter Values

Symbol	$\mathcal{R}_0 < 1$	Source	$\mathcal{R}_0 > 1$	Source	Unit
μ	$1{,}7 \times 10^{-4}$	Assumed	$1{,}7 \times 10^{-4}$	Assumed	1/day
β	$3{,}8 \times 10^{-5}$	Assumed	$8{,}5 \times 10^{-5}$	Ahmed et al., 2020	1/day
π	0,1960	WHO 2020	0,1960	WHO 2020	1/day
γ	0,07143	Tang et al., 2020	0,07143	Tang et al., 2020	1/day
σ	0,0054	Assumed	0,0054	Assumed	1/day
θ	0,25	Assumed	0,25	Assumed	1/day
δ	0,0667	Margenov et al., 2022	0,0667	Margenov et al., 2022	1/day
η	0,6200	Assumed	0,6200	Assumed	1/day
ξ	0,266	Singh et al., 2022	0,266	Singh et al., 2022	1/day

Population dynamics for $\eta = 0$ and $\eta = 0.62$

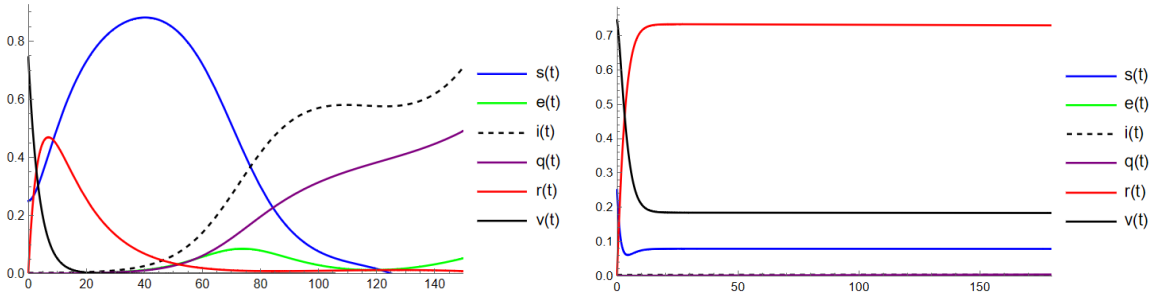

Figure 3. Population dynamics for $\eta = 0$ and $\eta = 0.62$

Figure 3 compares the condition when there is no proportion of the number vaccinated and the proportion of the number vaccinated of 62 percent. From the figure, when the proportion of vaccinated people is equal to zero, the system appears unstable as the susceptible subpopulation decreases over time, although there is an initial increase. In addition, the number of infected subpopulations will continue to increase indefinitely. In contrast, when the proportion of the number vaccinated is 0.62, the number of recovered subpopulations will increase. The number of infected subpopulations will decrease, the system in the figure shows a stable condition.

Population dynamics for $\mathcal{R}_0 < 1$ and $\eta = 0.62$

In the condition of $\mathcal{R}_0 < 1$, the system has one fixed point shown in the numerical solution according to the results obtained using Mathematica software calculations. $T_0(s, e, i, q, r, v) = (s^0, 0,0,0, r^0, v^0) = (0.0794; 0; 0; 0; 0.7356; 0.1849)$ is the disease-free fixed point that was determined by using the parameter values in Table 2 and having a value of $\mathcal{R}_0 \approx 0.4654$.

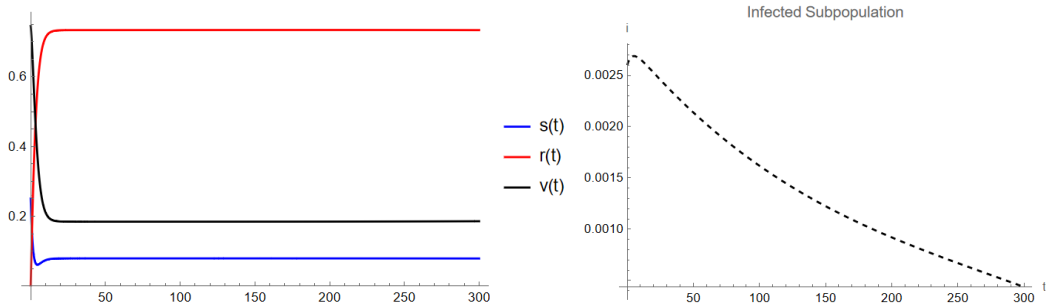

Figure 4. Population dynamics when $\mathcal{R}_0 < 1$

Figure 4 shows the dynamics of the subpopulations, where each subpopulation will go to the disease-free fixed point T_0 or be in a stable state around the fixed point T_0, in accordance with Theorem 1. Initially, the susceptible (s) and recovered (r) subpopulations decrease, then increase slightly and stabilize. Then, the infected subpopulation (i) increases slightly and then decreases.

Population dynamics for $\mathcal{R}_0 > 1$ and $\eta = 0.62$

In the condition of $\mathcal{R}_0 > 1$, the system has one fixed point shown in the numerical solution according to the results obtained using Mathematica software calculations. $T_1(s, e, i, q, r, v) = (s^*, e^*, i^*, q^*, r^*, v^*) = (0{,}0871; 0{,}0027; 0{,}0009; 0{,}0028; 0{,}7021; 0{,}2026)$ is the endemic fixed point that was determined by using the parameter values in Table 2 and having a value of $\mathcal{R}_0 \approx 1{,}04107$, as shown in Figure 5.

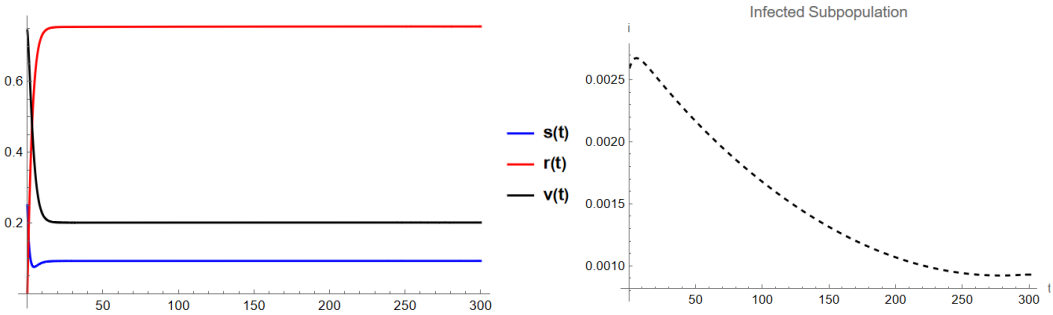

Figure 5. Population dynamics when $\mathcal{R}_0 > 1$

Figure 5 shows the subpopulation dynamics where each subpopulation will go to the endemic fixed point T_1 or in a stable state around the fixed point T_1 in accordance with Theorem 2. Initially, the susceptible (s) and recovered (r) subpopulations decrease, then increase slightly and stabilize. Then, the infected subpopulation (i) increased slightly and then decreased until it stabilized.

D. CONCLUSION AND SUGGESTIONS

This study is a development of the SEIR COVID-19 spread model with quarantine classes formed by Zeb. This model is modified by adding a vaccine subpopulation and the assumption that recovered individuals will become susceptible again, and the subpopulation that has been vaccinated will move to the recovered subpopulation. A disease-free fixed point that is locally asymptotically stable under the condition $\mathcal{R}_0 < 1$ and a disease-endemic fixed point that is

locally asymptotically stable under the condition $\mathcal{R}_0 > 1$ are the two fixed points that are obtained using this modified model. The results of a numerical simulation demonstrate outcomes that are consistent with the fixed point stability theorem.

Based on the numerical simulations that have been carried out, it is shown that to suppress the spread of COVID-19 in the city of Mataram, it is necessary to give a proportion of number vaccinated of 62% in accordance with government policy so that it can suppress the spread of the virus, or the infected subpopulation will decrease. Furthermore, giving the proportion of number vaccinated $\eta = 0.62$ will increase the recovered subpopulation. Therefore, the solution that can be used to control the spread of COVID-19 in the city of Mataram is by increasing the proportion of number vaccinated. In order to boost vaccination rates, the government can implement widespread education on the benefits of vaccination followed by equitable distribution of vaccines to all demographics. This model is applicable for various infectious diseases, yet it must still consider the assumptions or behaviors present in reality.

REFERENCES

Abidemi, A., Akanni, J. O., & Makinde, O. D. (2023). Healthcare Analytics A non-linear mathematical model for analysing the impact of COVID-19 disease on higher education in developing countries. *Healthcare Analytics*, *3*(May), 100193. https://doi.org/10.1016/j.health.2023.100193

Ahmed, I., Modu, G. U., Yusuf, A., Kumam, P., & Yusuf, I. (2020). A Mathematical Model of Coronavirus Disease (COVID-19) Containing asymptomatic symptomatic classes. *Results in Physics*, *21*(Feb), 103776. https://doi.org/10.1016/j.rinp.2020.103776

Bjørnstad, O. N., Shea, K., Krzywinski, M., & Altman, N. (2020). The SEIRS model for infectious disease dynamics. *Nature Methods*, *17(6)*,557–558. https://doi.org/10.1038/s41592-020-0856-2

Cao, J., Tu, W., Cheng, W., Yu, L., Liu, Y., Hu, X., & Liu, Q. (2020). *Clinical Features and Short-term Outcomes of 102 Patients with Coronavirus Disease 2019 in Wuhan , China*. *71(15), 748-755*. https://doi.org/10.1093/cid/ciaa243

Cheruku, V., Babu, B. S., Santhos, K., & Chlestina, G. (2023). Study of SEIQR mathematical model-prediction of spread of Covid-19. *AIP Conference Proceedings*, *2852*(1), 110002. https://doi.org/10.1063/5.0164809

DarAssi, M. H., Ahmad, I., Meetei, M. Z., Alsulami, M., Khan, M. A., & Tag-eldin, E. M. (2023). The impact of the face mask on SARS-CoV-2 disease: Mathematical modeling with a case study. *Results in Physics*, *51*(May), 106699. https://doi.org/10.1016/j.rinp.2023.106699

Diagne, M. L., Rwezaura, H., Tchoumi, S. Y., & Tchuenche, J. M. (2021). A Mathematical Model of COVID-19 with Vaccination and Treatment. *Computational and Mathematical Methods in Medicine*, *2021(9), 1250129*. https://doi.org/10.1155/2021/1250129

Hardianti, W. T., Sumarno, H., & Sianturi, P. (2022). Sensitivity Analysis of SEIRS Model with Quarantine on the Spread of Covid-19. *JTAM (Jurnal Teori Dan Aplikasi Matematika)*, *6*(4), 1034. https://doi.org/10.31764/jtam.v6i4.9627

Hassan, M. N., Mahmud, M. S., Nipa, K. F., & Kamrujjaman, M. (2023). Mathematical Modeling and COVID-19 Forecast in Texas, USA: A Prediction Model Analysis and the Probability of Disease Outbreak. *Disaster Medicine and Public Health Preparedness*, *17*(1), 21. https://doi.org/10.1017/dmp.2021.151

Khan, I. U., Hussain, A., Li, S., & Shokri, A. (2023). Modeling the Transmission Dynamics of Coronavirus Using Nonstandard Finite Difference Scheme. *Fractal and Fractional*, *7*(6), 1–16. https://doi.org/10.3390/fractalfract7060451

Margenov, S., Popivanov, N., Ugrinova, I., & Hristov, T. (2022). Mathematical Modeling and Short-Term Forecasting of the COVID-19 Epidemic in Bulgaria: SEIRS Model with Vaccination. *Mathematics*, *10*(15), 2570. https://doi.org/10.3390/math10152570

Ming, W.-K., Huang, J., & Zhang, C. J. P. (2020). Breaking down of healthcare system: Mathematical modelling for controlling the novel coronavirus (2019-nCoV) outbreak in Wuhan, China. *BioRxiv*,

January. 2020(1), 27. https://doi.org/10.1101/2020.01.27.922443

Naresh, R., Sundar, S., Verma, S. R., & Shukla, J. B. (2023). A mathematical model to study the spread of COVID-19 and its control in India. *Computational and Mathematical Biophysics*, *11*(1), 149. https://doi.org/10.1515/cmb-2022-0149

Nesteruk, I. (2020). Statistics-Based Predictions of Coronavirus Epidemic Spreading in Mainland China. *Innovative Biosystems and Bioengineering*, *4*(1), 13–18. https://doi.org/10.20535/ibb.2020.4.1.195074

Peter, O. J., Panigoro, H. S., Abidemi, A., Ojo, M. M., & Oguntolu, F. A. (2023). Mathematical Model of COVID-19 Pandemic with Double Dose Vaccination. *Acta Biotheoretica*, *71*(2), 19–20. https://doi.org/10.1007/s10441-023-09460-y

Pinto Neto, O., Kennedy, D. M., Reis, J. C., Wang, Y., Brizzi, A. C. B., Zambrano, G. J., de Souza, J. M., Pedroso, W., de Mello Pedreiro, R. C., de Matos Brizzi, B., Abinader, E. O., & Zângaro, R. A. (2021). Mathematical model of COVID-19 intervention scenarios for São Paulo—Brazil. *Nature Communications*, *12*(1), 1–13. https://doi.org/10.1038/s41467-020-20687-y

Polwiang, S. (2023). The lockdown and vaccination distribution in Thailand's COVID-19 epidemic: A model study. *Infectious Disease Modelling*, *8*(2), 551–561. https://doi.org/10.1016/j.idm.2023.05.002

Rahimi, I., Gandomi, A. H., Asteris, P. G., & Chen, F. (2021). Analysis and prediction of covid-19 using sir, seiqr and machine learning models: Australia, italy and uk cases. *Information (Switzerland)*, *12*(3), 1–25. https://doi.org/10.3390/info12030109

Rahmasari, S. M., Widowati, & Herdiana, R. (2023). Mathematical Modelling and Stability Analysis of the SEQIRD Model Spread of COVID-19. *AIP Publishing*, *2738*(1),140163. https://doi.org/10.1063/5.0140163

Resmawan, R., Yahya, L., Pakaya, R. S., Panigoro, H. S., & Nuha, A. R. (2022). Analisis Dinamik Model Penyebaran COVID-19 dengan Vaksinasi. *Jambura Journal of Biomathematics (JJBM)*, *3*(1), 29–38. https://doi.org/10.34312/jjbm.v3i1.13176

Salle, J. La, & Lefschetz, S. (1961). *Stability by Liapunov's Direct Method: With Applications* (4th ed.). Academic Press. https://onlinelibrary.wiley.com/doi/abs/10.1002/zamm.19620421022

Septiansyah, G., Karim, M. A., & Yulida, Y. (2022). *Pemodelan Matematika Penyebaran Covid-19 Dengan Model Sveir*. *16*(2), 101–116. https://10.20527/epsilon.v16i2.6496

Singh, A., Sapna, B., & Nivedita, D. (2022). Modelling and analysis of a SEIQR model on COVID - 19 pandemic with delay. *Modeling Earth Systems and Environment*, *8*(3), 3201–3214. https://doi.org/10.1007/s40808-021-01279-1

Van Den Driessche, P., & Watmough, J. (2002). Reproduction numbers and sub-threshold endemic equilibria for compartmental models of disease transmission. *Mathematical Biosciences*, *180*(1–2), 29–48. https://doi.org/10.1016/S0025-5564(02)00108-6

Verma, V., Agarwal, M., & Verma, A. (2023). A mathematical model for the novel coronavirus with effect of lockdown. *International Journal of Modeling, Simulation, and Scientific Computing*, *14(3),23500058*. https://doi.org/10.1142/S1793962323500058

Wang, F., Cao, L., & Song, X. (2022). Mathematical modeling of mutated COVID-19 transmission with quarantine, isolation and vaccination. *Mathematical Biosciences and Engineering*, *19*(8), 8035–8056. https://doi.org/10.3934/mbe.2022376

WHO. (2023). *Number of COVID-19 cases reported to WHO*. https://data.who.int/dashboards/covid19

Zeb, A., Alzahrani, E., Erturk, V. S., & Zaman, G. (2020). Mathematical Model for Coronavirus Disease 2019 (COVID-19) Containing Isolation Class. *BioMed Research International*, *2020*. 34(5), 2402. https://doi.org/10.1155/2020/3452402

Zhu, N., Zhang, D., Wang, W., Li, X., Yang, B., Song, J., Zhao, X., Huang, B., Shi, W., Lu, R., Niu, P., Zhan, F., Ma, X., Wang, D., Xu, W., Wu, G., Gao, G. F., & Tan, W. (2020). A Novel Coronavirus from Patients with Pneumonia in China, 2019. *New England Journal of Medicine*, *382*(8), 727–733. https://doi.org/10.1056/nejmoa2001017